



Assessment of Image Quality and Lesion Detectability With Digital PET/CT System

Olivier Delcroix¹, David Bourhis^{1,2,3}, Nathalie Keromnes¹, Philippe Robin^{1,2,3}, Pierre-Yves Le Roux^{1,2,3}, Ronan Abgral^{1,2,3}, Pierre-Yves Salaun^{1,2,3} and Solène Querellou^{1,2,3*}

OPEN ACCESS

¹ Nuclear Medicine Department, Brest University Hospital, Brest, France, ² EA 3878 GETBO IFR, Brest, France, ³ University of Bretagne Occidentale, Brest, France

Edited by:

Thomas Carlier,
Centre Hospitalier Universitaire (CHU)
de Nantes, France

Reviewed by:

Salvatore Annunziata,
Catholic University of the Sacred
Heart, Italy
Ronald Boellaard,
Amsterdam UMC, Netherlands
Joyce Van Sluis,
University Medical Center Groningen,
Groningen, Netherlands, in
Collaboration With Reviewer RB, Italy

*Correspondence:

Solène Querellou
solene.querellou@chu-brest.fr
orcid.org/0000-0002-4525-2696

Specialty section:

This article was submitted to
Nuclear Medicine,
a section of the journal
Frontiers in Medicine

Received: 13 November 2020

Accepted: 26 January 2021

Published: 22 February 2021

Citation:

Delcroix O, Bourhis D, Keromnes N,
Robin P, Le Roux PY, Abgral R,
Salaun PY and Querellou S (2021)
Assessment of Image Quality and
Lesion Detectability With Digital
PET/CT System.
Front. Med. 8:629096.
doi: 10.3389/fmed.2021.629096

Purpose: The aim of this study was to assess image quality and lesion detectability acquired with a digital Positron Emission Tomography/Computed Tomography (PET/CT) Siemens Biograph Vision 600 system.

Material and Methods: Consecutive patients who underwent a FDG PET/CT during the first week of use of a digital PET/CT (Siemens Biograph Vision 600) at the nuclear medicine department of the university hospital of Brest were analyzed. PET were realized using list mode acquisition. For all patients, 4 datasets were reconstructed. We determined, according to phantom measurements, an equivalent time acquisition/reconstruction parameters pair of the digital PET/CT corresponding to an analog PET/CT image quality (“analog-like”) as reference dataset. We compared the reference dataset with 3 others digital PET/CT reconstruction parameters, allowing a decrease of emission duration: 60, 90, and 120 s per bed position. Three nuclear medicine physicians evaluated independently, for each dataset, overall image quality [Maximal Intensity Projection (MIP), noise, sharpness] using a 4-point scale. Physicians assessed also lesion detection capability by reporting new visible lesions on each digital datasets with their confidence level in comparison with analog-like dataset.

Results: Ninety-eight patients were analyzed. Image quality of MIP (IQ_{MIP}), sharpness (IQ_{SHARPNESS}), and noise (IQ_{NOISE}) of all digital datasets (60, 90, and 120 s) were better than those evaluated with analog-like reconstruction. Moreover, digital PET/CT system improved IQ_{MIP}, IQ_{NOISE}, and IQ_{SHARPNESS} whatever the BMI. Lesion detection capability and confidence level were higher for 60, 90, 120 s per bed position, respectively, than for analog-like images.

Conclusion: Our study demonstrated an improvement of image quality and lesion detectability with a digital PET/CT system.

Keywords: analog detectors, PET/CT, clinical evaluation, image quality, SiPM

INTRODUCTION

Positron emission tomography/computed tomography (PET/CT) is a widely used multimodality imaging method that provides metabolic information for oncological and non-oncological disease management (1). Steady improvements in detector design and architecture, as well as implementation of time-of-flight (TOF) and point spread function (PSF) correction technology, have led to significant improvements in sensitivity and image quality (2–5). New type of PET detectors, silicon photomultiplier (SiPM)-based detectors, has been recently developed (6–8) as a key innovation replacing conventional photomultipliers (PMT). Integration of SiPM in PET/CT scanners enabled the development of digital PET/CT scanners, replacing conventional analog PET/CT scanners. The technology, based on semi-conductor detector called SPAD (single photon avalanche diode), has better detection characteristics than PMT. Firstly, if individual SPAD are as sensitive as PMT, SPAD can cover the whole surface of scintillation crystal and the global sensitivity is higher. Secondly, SiPM are faster than PMT, resulting to a time resolution of 215 ps for Siemens Vision PET/CT system (9). The improvement in time resolution lead to more efficient TOF reconstructions with a very fast convergence and noiseless images (10) with high effective sensitivity in regards to PMT systems. Moreover, the sensitivity improvement gave the opportunity to design smaller crystal pixels leading to a better spatial resolution. Based on phantom studies that were recently published using digital PET systems (6, 11), it has been demonstrated that digital PET outperforms analog PET in terms of spatial resolution and sensitivity. However, to our knowledge, data on the comparison of digital PET and analog PET in terms of image quality

and diagnostic confidence in patients undergoing PET/CT is scarce (12–14).

The aim of our study was to assess the overall image quality and lesion detection capability improvement in patients undergoing digital PET/CT scanning on a Siemens Biograph Vision 600.

MATERIALS AND METHODS

Patients

All consecutive patients referred for an ^{18}F -Fluoro-Deoxy-Glucose (FDG) PET/CT for oncological or non-oncological purpose during the first week of use of the Biograph Vision 600 (Siemens Healthineers, Knoxville, TN, United States) at the nuclear medicine department of Brest university hospital, from Oct 10, 2018 were included. All procedures performed in this study were in accordance with the ethical standards of the institutional research committee on human experimentation and with the Helsinki Declaration of 1975, as revised in 2008. The ethics committee of Brest University Hospital reviewed and approved the protocol of our retrospective study (approval number B2020CE.22). All patients provided written informed consent.

PET/CT Characteristics

Two PET/CT systems were used: the analog Biograph mCT Flow equipped with extended axial Field Of View (FOV) TrueV and the digital Biograph Vision 600 (Siemens Healthineers, Knoxville, TN, United States).

CT acquisitions and reconstruction parameters were similar for both systems: helical CT acquisition, with iodine contrast when it was possible, was firstly performed for attenuation

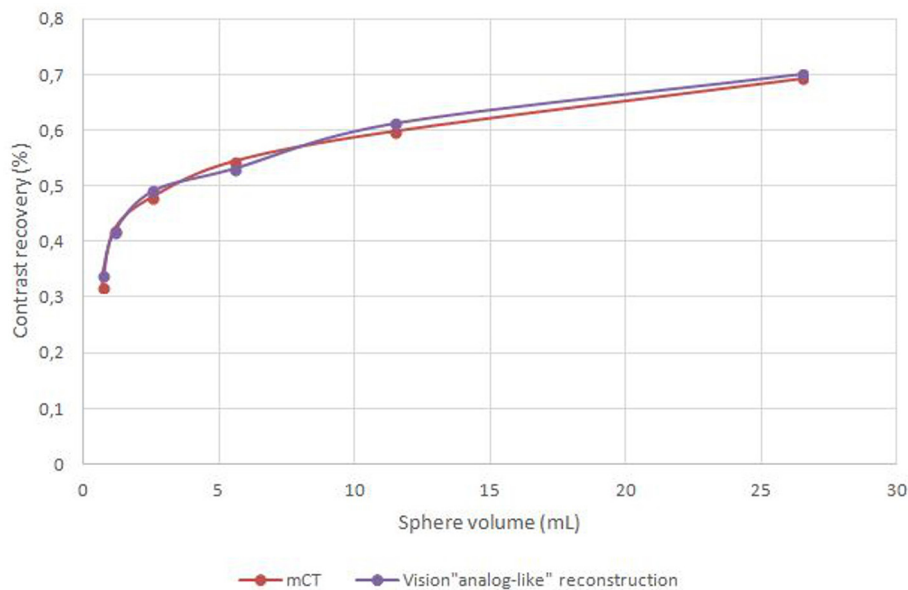


FIGURE 1 | Contrast recovery measured on original Biograph mCT images and on Biograph Vision "Analog like" images.

correction and anatomic localization. CT parameters were 110 kVp (automatic kV modulation, carekV[®]); 80 refmAs with automatic dose modulation (care4D[®]); 0.5 second rotation time; 19.2 mm total collimation width; pitch 1, 512 matrix size, 0.98 × 0.98 mm pixels; 2 mm slices thickness.

PET data was acquired in 3D list mode during 120 s per bed position. Axial FOV were 218 and 263 mm and overlap fraction were 43 and 49%, respectively, for Biograph mCT and Biograph Vision.

Images acquired on the Biograph mCT TrueV were reconstructed in daily practice. The reconstruction matrix and voxels size were, respectively, 200 × 200 and 4 × 4 × 2 mm and the reconstruction algorithm was OSEM3D with application of TOF and resolution modeling, 2 iterations, 21 subsets, and 2 mm Gaussian post filtering.

Images acquired on the Biograph Vision 600 were reconstructed in daily practice. The reconstruction matrix and voxels size were, respectively, 440 × 440 and 1.65 × 1.65 × 1.65 mm and the reconstruction algorithm was OSEM3D with application of TOF and resolution modeling, 4 iterations, 5 subsets, and 2 mm Gaussian post filtering.

Phantom PET/CT Preclinical Study

In order to avoid undergoing 2 consecutive PET/CT on 2 different systems (analog and digital systems) for the evaluation of image quality and lesion detectability, we performed a preclinical study using phantom filled with FDG. Phantom was scanned on both analog and digital systems to estimate the acquisition and reconstruction parameters providing an image quality comparable to an analog system (“Analog-like”) acquired on digital PET/CT and then used these data for the clinical study with a single acquisition on a digital PET/CT system alone.

So, we determined, according to phantom measurements, an equivalent time acquisition/reconstruction parameters pair of the digital PET/CT Biograph Vision 600 corresponding to an analog PET/CT image quality (“analog-like”) of the Biograph mCT TrueV as reference.

A NEMA IEC phantom, filled with 5 MBq/L in the background compartment and 20 MBq/L in the spheres (diameters were, respectively, 13, 17, 21, 28, and 37 mm), was both scanned on a Biograph mCT and a Biograph Vision during 120 s in list-mode. According to the literature, NEMA phantom measurements on Biograph mCT and on Biograph Vision systems demonstrated a sensitivity ratio of 1.6 (11, 15). TOF effective sensitivity gain ratio was estimated by $\Delta t_{mCT}/\Delta t_{Vision} = 2.5$ (16). Thus, the overall sensitivity ratio between Biograph mCT and Biograph Vision is $\sim 1.6 \times 2.5 = 4$, allowing to determine 30 s emission time per bed position for the Biograph Vision in comparison with 120 s for the Biograph mCT. On this basis, multiple reconstruction parameters were tested on the Biograph Vision and compared to the results obtained with the Biograph mCT. On reconstructed images, Contrast Recovery (CR) was calculated as the ratio of the image contrast (ratio of mean intensity in spheres and mean intensity in background) and the radioactivity contrast (4:1). Analog-like reconstruction parameters on the Biograph Vision were selected in order to simulate an equivalent CR on the Biograph mCT.

We also determined the reconstruction parameters that would allow to perform 60 and 90 s per bed position compared to the daily practice reference on Biograph Vision (120 s per bed position, matrix of 440 × 440 with voxels size of 1.65 × 1.65 × 1.65 mm, OSEM3D with application of TOF and resolution modeling, 4 iterations, 5 subsets, and 2 mm Gaussian post filtering).

Multiple reconstructions were performed and signal to noise ratio (SNR) was calculated as the ratio of the standard deviation and the mean intensity value in six regions of interest in the background area. Sixty and ninety seconds protocols reconstruction parameters were determined in such a way that SNR was at least equivalent to the daily

TABLE 1 | Vision reconstruction parameters and the corresponding SNR.

Frame duration	Parameters	SNR
Analog like	3.3 × 3.3 × 1.65 mm voxels, 5 iterations, 5 subsets, 4 mm Gaussian filter	10.8
60 s	1.65 × 1.65 × 1.65 mm voxels, 3 iterations, 5 subsets, 3 mm Gaussian filter	9.7
90 s	1.65 × 1.65 × 1.65 mm voxels, 3 iterations, 5 subsets, 2 mm Gaussian filter	9.6
120 s	1.65 × 1.65 × 1.65 mm voxels, 4 iterations, 5 subsets, 2 mm Gaussian filter	9

TABLE 2 | Patients characteristics.

Characteristics	No. of patients (%) (n = 98)
Age (years)	
Mean ± SD	64 ± 13
Median (range)	65 (19–88)
Sex—no. (%)	
Male	58 (59%)
Female	40 (41%)
Weight (kg)	
Mean ± SD	73 ± 19
Median (range)	70 (45–140)
BMI	
Mean ± SD	25.5 ± 6.1
Median (range)	24.3 (15.6–49.6)
FDG activity injected (MBq)	
Mean ± SD	222 ± 58
Median (range)	212 (134–425)
Delay between injection and acquisition (min)	
Mean ± SD	61.2 ± 5.7
Median (range)	60 (55–94)
Glucose blood level (mmol/L)	
Mean ± SD	5.9 ± 1
Median (range)	5.7 (4.3–10.4)
Iodine contrast CT—no. (%)	
Yes	63 (64%)
No	35 (36%)

practice reference reconstruction and images as sharp as possible.

Patients PET/CT Clinical Study

Prior to radiotracer injection, all patients fasted for at least 6 h and then were injected with standard activity of ^{18}F -FDG (3 MBq/kg). Approximately 60 min after FDG injection (17), patients underwent a list-mode PET/CT imaging protocol only on the Biograph Vision. PET data was reconstructed according to “analog-like,” 60, 90, and 120 s protocols.

Image Analysis

Images were reviewed using a dedicated workstation (Syngovia, VB30, Siemens Healthineers) with 4 PET datasets

opened and linked automatically for their simultaneous assessment. Image quality was assessed independently by three experienced nuclear medicine physicians (OD, NK, and SQL with two, 8 and 15 years of experience in PET reading, respectively). Interpreters were blinded of all clinical data but were aware of the subset of reconstruction data (“analog-like” dataset, 60, 90, and 120 s per bed position digital datasets). Analysis of image quality was performed in two steps.

The first step was an overall qualitative assessment using a four-point scale (ranging from a score of 1 [excellent quality maximum intensity projection (MIP)] to 4 [poor quality MIP]) (18). The 4 datasets were subsequently compared side by side for noise and sharpness with the same scale (18). Previous criteria

TABLE 3 | Data of overall qualitative assessment (MIP, noise, and sharpness) according to readers.

	Reader 1		Reader 2		Reader 3		Total		<i>p</i>
	Mean-value	<i>SD</i>	Mean-value	<i>SD</i>	Mean-value	<i>SD</i>	Mean-value	<i>SD</i>	
MIP									
Analog like	2.14	0.41	2.44	0.54	2.34	0.48	2.31	0.49	
60 s	1.16	0.40	1.46	0.54	1.26	0.44	1.29	0.48	<0.0001
90 s	1.11	0.35	1.10	0.30	1.14	0.35	1.12	0.33	<0.0001
120 s	1.09	0.32	1.08	0.28	1.13	0.34	1.10	0.31	<0.0001
Noise									
Analog like	2.20	0.45	2.51	0.60	2.33	0.51	2.35	0.54	
60 s	1.19	0.42	1.39	0.57	1.19	0.40	1.26	0.48	<0.0001
90 s	1.10	0.34	1.12	0.33	1.09	0.29	1.11	0.32	<0.0001
120 s	1.11	0.32	1.18	0.41	1.17	0.38	1.16	0.37	<0.0001
Sharpness									
Analog like	2.86	0.35	2.31	0.51	2.48	0.50	2.55	0.51	
60 s	1.91	0.29	1.88	0.39	1.56	0.50	1.78	0.43	<0.0001
90 s	1.78	0.42	1.13	0.34	1.18	0.39	1.36	0.48	<0.0001
120 s	1.04	0.20	1.05	0.22	1.07	0.26	1.05	0.23	<0.0001

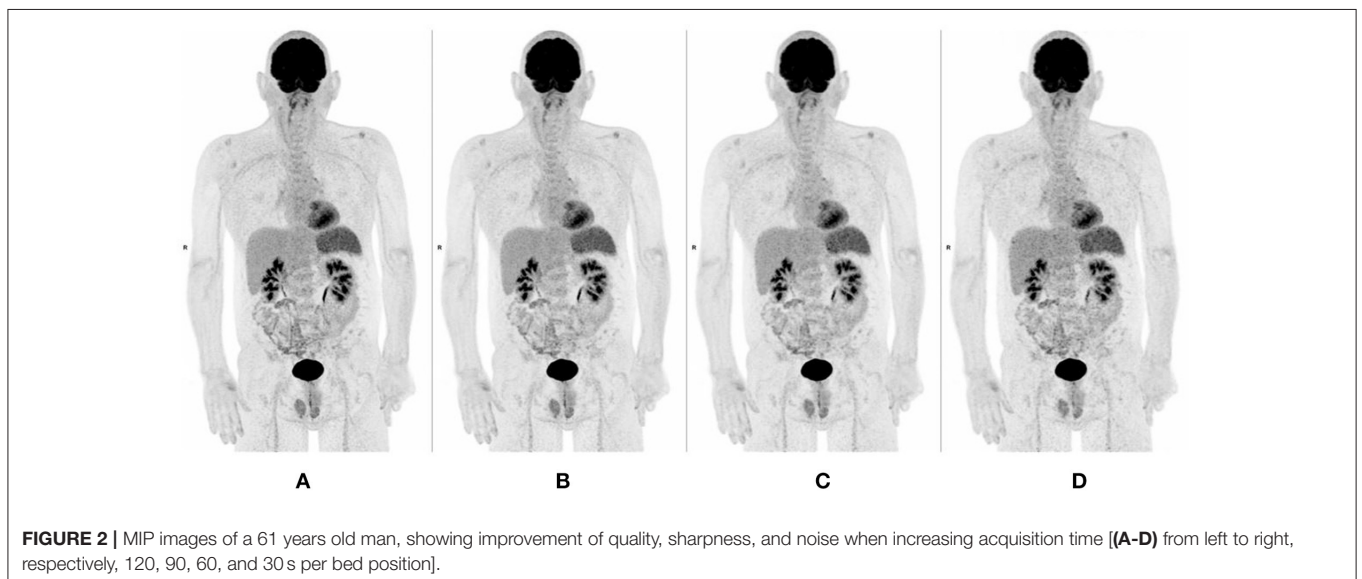


FIGURE 2 | MIP images of a 61 years old man, showing improvement of quality, sharpness, and noise when increasing acquisition time [(A-D) from left to right, respectively, 120, 90, 60, and 30 s per bed position].

were also classified according to body mass index (BMI) for each PET datasets on the basis of the patient's BMI (BMI < 25 kg/m²; BMI > 25 kg/m²).

The second step consisted for each physician to identify any new FDG uptake in each digital dataset, in comparison with the "analog-like" dataset. For each uptake identified, physicians gave their confidence level according to a four-point scale (1[high confidence] to 4[low confidence]).

Statistical Analysis

Each parameter (overall quality of MIP, noise, and sharpness) was calculated for each reader and for all readers [mean +/- standard deviation (SD)] according to reconstruction datasets and on the basis of patients' BMI.

Data is presented as mean values +/- SD. The Wilcoxon test was used to compare data according

to each reconstruction and BMI subgroups (BMI < 25 kg/m²; BMI > 25 kg/m²). A $p < 0.05$ was considered statistically significant. Statistical analysis was performed using XLSTAT-Life software (Addinsoft, Paris, France).

RESULTS

Phantom Study

The reconstruction parameters which produced the best Analog like reconstruction were $3.3 \times 3.3 \times 1.65$ mm voxels, 5 iterations, 5 subsets and 4 mm Gaussian post filtering. CR measured on original Biograph mCT images and Analog like Biograph Vision reconstruction are shown in **Figure 1**.

Reconstruction parameters and the corresponding SNR are detailed in **Table 1**.

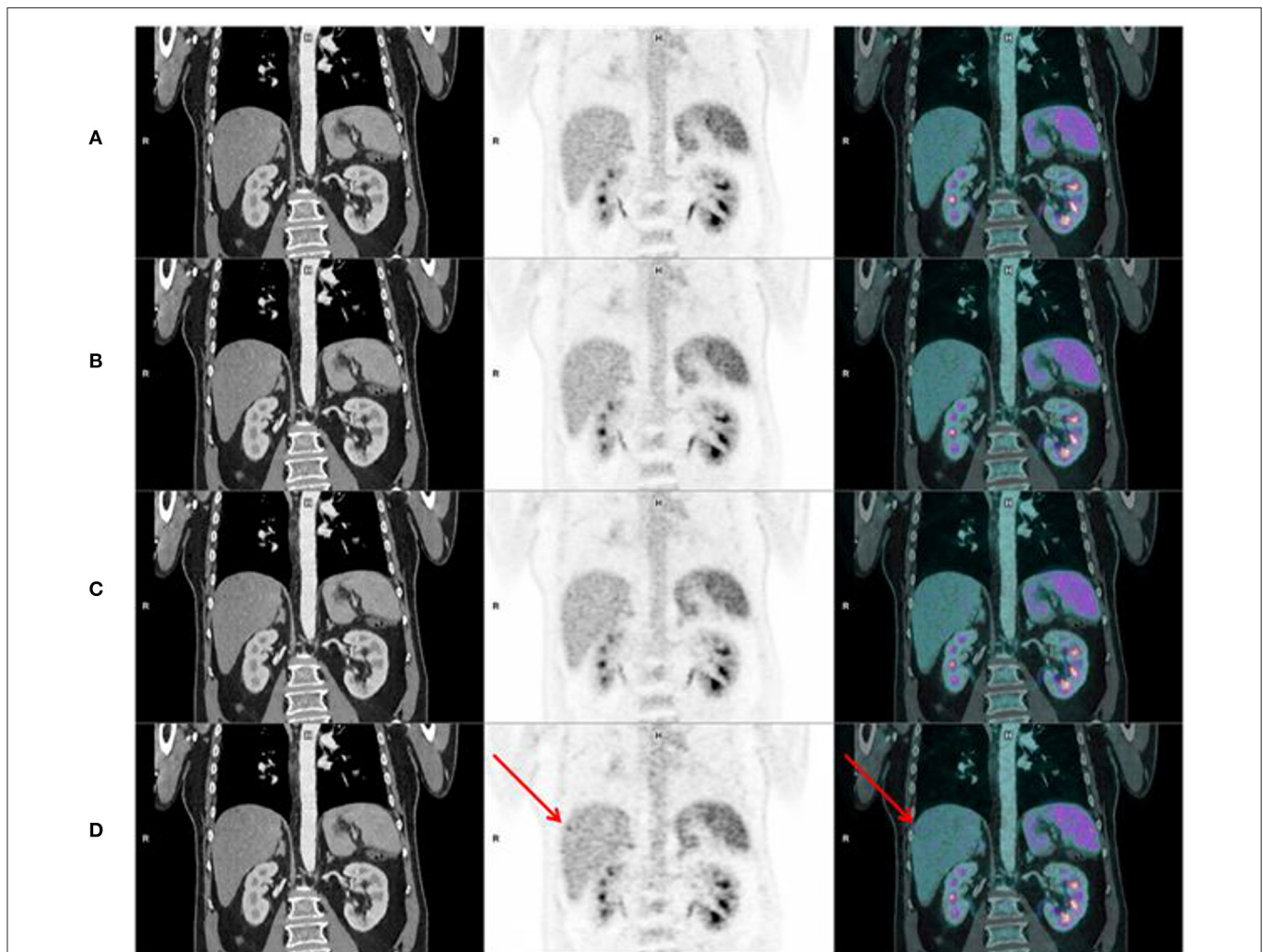


FIGURE 3 | Coronal CT, PET, and fusion images in the same patient, showing better sharpness of organs, pyelo-ureteral uptakes, and less hepatic noise when increasing acquisition time [(A-D) from top to bottom, respectively, 120, 90, 60, and 30 s per bed position]. We can see noise on the "Analog-like" acquisition which can mimic focal uptake in the right liver (arrow), and which disappears on the other acquisitions.

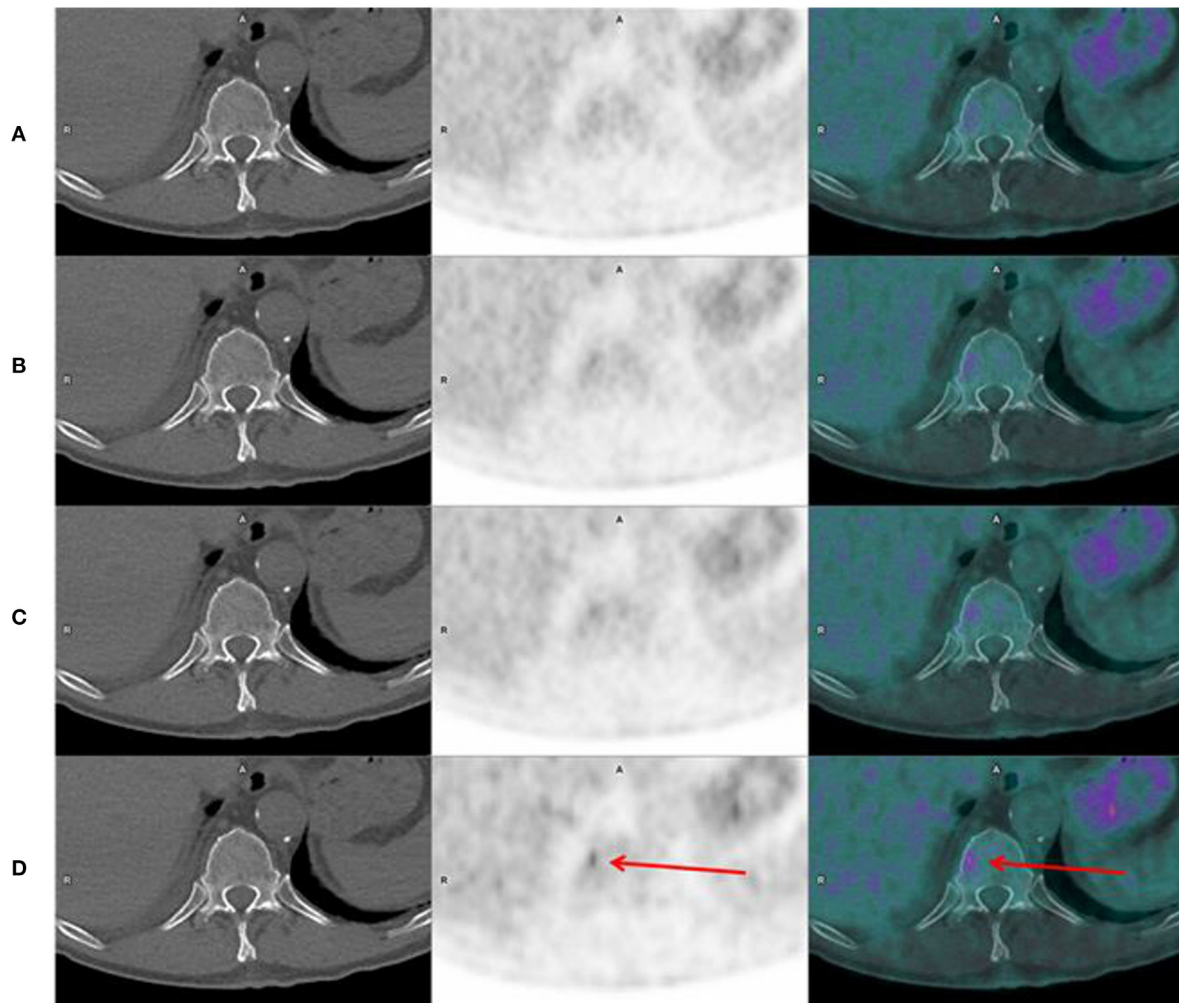


FIGURE 4 | Axial CT, PET, and fusion images in a 65 years old man, showing a bone focal uptake in T11, on the “Analog-like” acquisition, which disappears when increasing acquisition time, and corresponding actually to noise [(A-D) from top to bottom, respectively, 120, 90, 60, and 30 s per bed position].

Patients Study

Ninety-nine patients were included. One patient was excluded from the analysis because of missing data.

Characteristics of the remaining 98 patients are summarized in **Table 2**.

Whole-Body Image Quality Analysis

Data of overall qualitative assessment (MIP, noise, and sharpness) is detailed below in **Table 3**.

For all readers, image quality of MIP (IQ_{MIP}), sharpness ($IQ_{SHARPNESS}$), and noise (IQ_{NOISE}) of all digital datasets (60, 90, and 120 s per bed position) were better than those evaluated with “analog-like” reconstruction: MIP was 1.10 ± 0.31 for the 120 s per bed position dataset as compared with 2.31 ± 0.49 for the “analog-like” dataset. Longer acquisition duration per bed position was associated

with better IQ_{MIP} and $IQ_{SHARPNESS}$ indices as illustrated in **Figures 2–4**.

The analysis according to BMI ($BMI < 25 \text{ kg/m}^2$, $BMI > 25 \text{ kg/m}^2$) is described below in **Table 4**.

In BMI subgroups IQ_{MIP} , $IQ_{SHARPNESS}$, and IQ_{NOISE} improved with the acquisition duration except for three comparisons. These results are detailed below in **Table 5**.

IQ_{MIP} was not statistically better for the 120 s reconstruction dataset than for the 90 s reconstruction dataset in patients with $BMI > 25 \text{ kg/m}^2$. IQ_{NOISE} was not statistically better for the 120 s reconstruction dataset than for the 90 s reconstruction dataset in patients with $BMI < 25 \text{ kg/m}^2$ and IQ_{NOISE} was statistically better for the 90 s reconstruction dataset than for the 120 s reconstruction dataset for patients with $BMI > 25 \text{ kg/m}^2$.

According to dichotomy BMI analysis under or over 25 kg/m^2 , IQ_{MIP} , IQ_{NOISE} and $IQ_{SHARPNESS}$ were better for patients with a $BMI < 25 \text{ kg/m}^2$ than for patients with a $BMI > 25 \text{ kg/m}^2$,

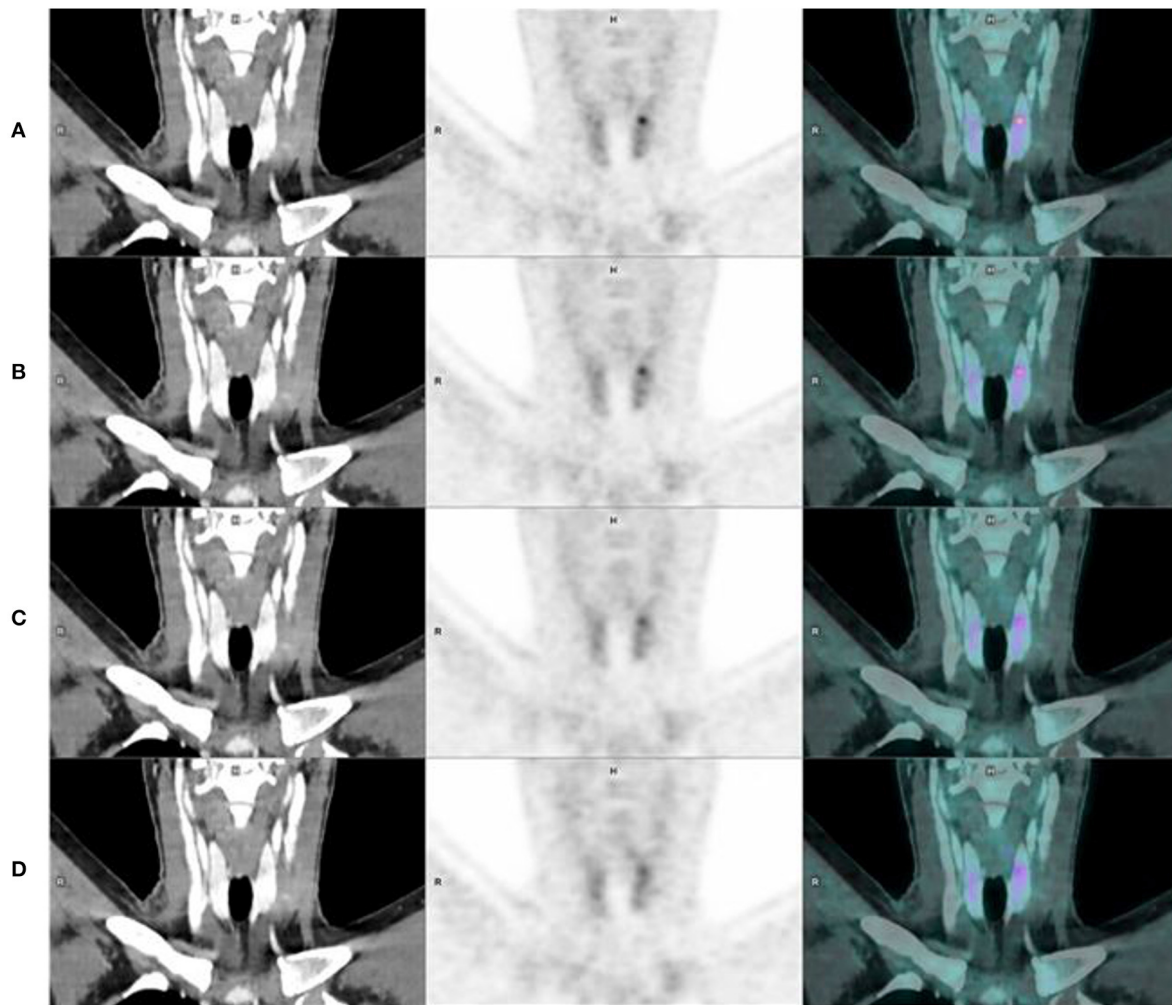


FIGURE 5 | Coronal CT, PET, and fusion images in a 48 years old woman, illustrating detectability improvement when increasing acquisition time, with appearance of a focal uptake in left thyroid lobe, which cannot be seen on the “Analog-like” acquisition [(A-D) from top to bottom, respectively, 120, 90, 60, and 30 s per bed position].

for all reconstruction datasets. These results are detailed below in **Table 6**.

$IQ_{SHARPNESS}$ was not statistically different between the 60 and the 90 s reconstruction datasets ($p = 0.284$ and $p = 0.311$, respectively).

Lesion Detectability

The detectability improved progressively with the acquisition per bed position duration as illustrated in **Figures 4, 5**. These results are presented below in **Table 7**.

Longer the acquisition step bed duration was, higher was the number of detected lesions. The confidence index improved also progressively with the acquisition bed position duration.

DISCUSSION

Our study showed that digital PET/CT provides improved image quality and outperforms analog PET/CT, especially for MIP,

sharpness, and noise with increased detectability at equal or less acquisition duration and injected activity. Up to date, only few studies evaluated in clinical practice, the differences of image quality and lesion detectability between digital and analog PET/CT systems. According to phantom measurements, several studies highlighted a quality improvement of digital PET/CT on a variety of commercial systems: Discovery MI (8), Vereos (6), and Vision (11). Gnesin et al. (19) compared the image quality in 5 PET/CT systems (3 digital PET/CT and 2 analog devices) and reported that a comparable image quality is achievable with a TAP [time (min) * mass activity (MBq/kg) product] reduction of 40% with digital PET/CT. Moreover, the authors suggested that digital PET systems potentially lead to lesions detectability improvement. We assumed in our study a time reduction factor of 4 between Biograph mCT and Biograph Vision. This was consistent with previous articles on phantom studies: indeed, Carlier et al. (20), Gnesin et al. (19), and Surti et al. (21) proposed, respectively, a reduction factor of 2.8

TABLE 4 | Data of overall qualitative assessment (MIP, noise, and sharpness) according to BMI (< or > 25 kg/m²).

	BMI < 25 (56 patients)			BMI >25 (42 patients)		
	Mean-value	SD		Mean-value	SD	
MIP						
Analog like	2.19	0.41		2.46	0.54	
60 s	1.19	0.41		1.43	0.53	
90 s	1.08	0.29		1.17	0.37	
120 s	1.04	0.22		1.19	0.39	
Noise						
Analog like	2.17	0.41		2.58	0.59	
60 s	1.15	0.36		1.40	0.57	
90 s	1.04	0.19		1.19	0.42	
120 s	1.05	0.21		1.30	0.48	
Sharpness						
Analog like	2.48	0.50		2.64	0.51	
60 s	1.74	0.44		1.79	0.45	
90 s	1.34	0.47		1.39	0.49	
120 s	1.03	0.17		1.09	0.28	

TABLE 5 | Statistical analysis of parameters (MIP, noise, and sharpness) according to datasets for patients under or over 25 kg/m².

		MIP			Noise			Sharpness		
		Analog like	60	90	Analog like	60	90	Analog like	60	90
BMI < 25 56 patients	Analog like									
	60	<0.0001			<0.0001			<0.0001		
	90	<0.0001	<0.0001		<0.0001	<0.0001		<0.0001	<0.0001	
BMI > 25 42 patients	120	<0.0001	<0.0001	0.0078	<0.0001	<0.0001	0.4237	<0.0001	<0.0001	<0.0001
	Analog like									
	60	<0.0001			<0.0001			<0.0001		
BMI > 25 42 patients	90	<0.0001	0.0004		<0.0001	<0.0001		<0.0001	<0.0001	
	120	<0.0001	0.0009	0.1489	<0.0001	0.0004	0.0004	<0.0001	<0.0001	<0.0001

between a Vision 450 and a mCT, 3.12 and 4–6 between a Vision 600 and a mCT, respectively. Nevertheless, the extrapolation of phantom data remains anyways difficult in human clinical daily practice and only few studies have evaluated the clinical impact of digital PET/CT system in patients. Lopez-Mora et al. (22) compared image quality and lesion detection capability between a digital and an analog PET/CT system. One hundred patients sequentially underwent both a digital and an analog PET/CT with a mean delay of 50 +/- 14 min between the two image acquisitions. The digital system allowed a significantly better image quality and a greater lesion detectability than the analog system. In the same cohort, Fuentes-Ocampo et al. (23) assessed whether digital PET/CT impacts the quantification of SUV_{max} in target lesions and in reference regions (liver and mediastinal blood pool) in comparison to analog PET/CT. They concluded that SUV_{max} of target lesions and mediastinal blood pool measured by the digital system were significantly higher than those obtained by the analog one whereas liver mean SUV_{max} did not differ between the two PET/CT systems. More recently, van Sluis et al. (24) evaluated the image quality

and semiquantitative analysis between a digital PET/CT system (Biograph Vision) and its analog predecessor (Biograph mCT). The authors concluded that the Biograph Vision outperforms the Biograph mCT in terms of image quality, lesion demarcation, and signal-to-noise ratio without any significant difference in semiquantitative assessment in a population of 20 patients. Lately, Kim et al. (25) confirmed also in a small cohort (30 patients) that digital PET/CT (Discovery MI; GE Healthcare) provides improved image quality and lesion detectability compared to a standard PET/CT (Biograph mCT, Siemens Healthineers). The mean time delay between both scans was shorter than that in Van Sluis study (17 vs. 37 min) (24, 25). The authors stressed as limitation of their studies the impossibility of performing both acquisitions at the same time and especially the impossibility of taking into account the evolution of FDG biodistribution between the two acquisitions (23, 24). In order to overcome this limitation, we analyzed 4 PET datasets acquired at the same time. We also evaluated the improvement of image quality according to BMI. Indeed in a recent study published by Hatami et al. (26), the authors concluded that the most impactful difference in

TABLE 6 | Statistical analysis of parameters (MIP, noise, and sharpness) according to BMI for all datasets.

	BMI <25 vs. BMI >25								
	MIP			Noise			Sharpness		
	<25	>25	<i>p</i>	<25	>25	<i>p</i>	<25	>25	<i>p</i>
Analog like (30)	2.19	2.46	<0.0001	2.17	2.58	<0.0001	2.48	2.64	0.007
60	1.19	1.43	<0.0001	1.15	1.40	<0.0001	1.74	1.79	0.284
90	1.08	1.17	0.019	1.04	1.20	<0.0001	1.34	1.40	0.311
120	1.04	1.19	<0.0001	1.05	1.30	<0.0001	1.03	1.09	0.032

TABLE 7 | Analysis of new uptake and confidence level of all readers according to datasets.

Dataset	Physicians (SQ, OD, and NK)	
	All new uptake (vs. Analog-like)	Confidence Level
60 s	146	2.38
90 s	189	1.85
120 s	201	1.49

scan time, dosimetry and FDG dose was observed in overweight patients. Moreover, we found in our cohort that, whatever the BMI, digital PET/CT system improved the image quality.

Thanks to an improved image quality and a better detectability, the use of digital PET/CT is expected to improve patient management enabling better characterization and detection of lesions previously unseen when using analog systems (27). The improvement of the confidence index described in our study could particularly lead to a decrease in the proportion of uptakes deemed equivocal. The increase of detected lesions might lead as well to improve staging accuracy and prognostic value, by example an earlier diagnosis of small metastatic lesions.

In the other hand, while image quality and detectability is improved by digital PET systems with an equal or reduced acquisition duration, this improvement could probably be used as well to optimize administered activity. Indeed in clinical practice, taking into account particular circumstances (screening, pediatric population, painful patient, claustrophobia, etc.), these improvements have to be considered to determine the most optimized image quality with the lowest radiation and shortest acquisition duration.

Our study presents some limitations. Firstly, we compared three digital datasets to an “analog-like” dataset, which was actually a simulated analog dataset. This “analog-like” dataset may differ slightly from an actual analog system. However, we performed a phantom study in order to minimize the differences between the analog and the analog-like images and validate the analog-like reference. Secondly, physicians who reviewed all PET reconstructions read all 4 datasets simultaneously and knew

which parameters were used for each dataset. This could have impacted the assessment of quality indices, by directly comparing all datasets together. Finally, the clinical impact of new uptakes or lesions that were detected only on highest quality images cannot be determined in this study.

CONCLUSION

In summary, our study demonstrated in a large cohort an improvement of image quality and lesion detectability with a digital PET/CT system. Future studies should assess the impact of these changes on clinical management.

DATA AVAILABILITY STATEMENT

The raw data supporting the conclusions of this article will be made available by the authors, without undue reservation.

ETHICS STATEMENT

The studies involving human participants were reviewed and approved by the ethics committee of Brest University Hospital reviewed and approved the protocol of our retrospective study (approval number B2020CE.22). All patients provided written informed consent. The patients/participants provided their written informed consent to participate in this study.

AUTHOR CONTRIBUTIONS

OD, NK, and SQ interpreted the different PET/CT. DB performed all the reconstructions. NK prepared tables and figures. OD performed the statistical analysis. SQ wrote the manuscript. PYS and SQ designed the study. RA, PYLR, and PR corrected the manuscript. All authors contributed to the article and approved the submitted version.

ACKNOWLEDGMENTS

We thank G. Le Gal MD, Ph.D., for his invaluable comments and suggestions regarding this work.

REFERENCES

- Schoder H, Erdi YE, Larson SM, Yeung HW. PET/CT: a new imaging technology in nuclear medicine. *Eur J Nucl Med Mol Imaging*. (2003) 30:1419–37. doi: 10.1007/s00259-003-1299-6
- Surti S, Kuhn A, Werner ME, Perkins AE, Kolthammer J, Karp JS. Performance of Philips Gemini TF PET/CT scanner with special consideration for its time-of-flight imaging capabilities. *J Nucl Med*. (2007) 48:471–80.
- Karp JS, Surti S, Daube-Witherspoon ME, Muehllehner G. Benefit of time-of-flight in PET: experimental and clinical results. *J Nucl Med*. (2008) 49:462–70. doi: 10.2967/jnumed.107.044834
- Surti S. Update on time-of-flight PET imaging. *J Nucl Med*. (2015) 56:98–105. doi: 10.2967/jnumed.114.145029
- Wright CL, Binzel K, Zhang J, Knopp MV. Advanced functional tumor imaging and precision nuclear medicine enabled by digital PET technologies. *Contrast Media Mol Imaging*. (2017) 2017:5260305. doi: 10.1155/2017/5260305
- Rausch I, Ruiz A, Valverde-Pascual I, Cal-Gonzalez J, Beyer T, Carrio I. Performance evaluation of the Philips Vereos PET/CT system according to the NEMA NU2-2012 standard. *J Nucl Med*. (2018) 60:561–7. doi: 10.2967/jnumed.118.215541
- Zhang J, Maniawski P, Knopp MV. Performance evaluation of the next generation solid-state digital photon counting PET/CT system. *EJNMMI Res*. (2018) 8:97. doi: 10.1186/s13550-018-0448-7
- Hsu DFC, Ilan E, Peterson WT, Uribe J, Lubberink M, Levin CS. Studies of a next-generation silicon-photomultiplier-based time-of-flight PET/CT system. *J Nucl Med*. (2017) 58:1511–8. doi: 10.2967/jnumed.117.189514
- Hutton; BF. Advances in clinical molecular imaging instrumentation. *Clin Transl Imaging*. (2018) 6:31–45. doi: 10.1007/s40336-018-0264-0
- Surti S, Karp JS. Advances in time-of-flight PET. *Phys Med*. (2016) 32:12–22. doi: 10.1016/j.ejmp.2015.12.007
- van Sluis JJ, de Jong J, Schaar J, Noordzij W, van Snick P, Dierckx R, et al. Performance characteristics of the digital biograph vision PET/CT system. *J Nucl Med*. (2019) 60:1031–6. doi: 10.2967/jnumed.118.215418
- Sonni I, Baratto L, Park S, Hatami N, Srinivas S, Davidzon G, et al. Initial experience with a SiPM-based PET/CT scanner: influence of acquisition time on image quality. *EJNMMI Phys*. (2018) 5:9. doi: 10.1186/s40658-018-0207-x
- Nguyen NC, Vercher-Conejero JL, Sattar A, Miller MA, Maniawski PJ, Jordan DW, et al. Image quality and diagnostic performance of a digital PET prototype in patients with oncologic diseases: initial experience and comparison with analog PET. *J Nucl Med*. (2015) 56:1378–85. doi: 10.2967/jnumed.114.148338
- van Sluis J, Boellaard R, Dierckx R, Stormezand GN, Glaudemans A, Noordzij W. Image quality and activity optimization in oncologic (18)F-FDG PET using the digital biograph vision PET/CT system. *J Nucl Med*. (2020) 61:764–71. doi: 10.2967/jnumed.119.234351
- Karlberg AM, Saether O, Eikenes L, Goa PE. Quantitative comparison of PET performance-Siemens biograph mCT and mMR. *EJNMMI Phys*. (2016) 3:5. doi: 10.1186/s40658-016-0142-7
- Conti M. State of the art and challenges of time-of-flight PET. *Phys Med*. (2009) 25:1–11. doi: 10.1016/j.ejmp.2008.10.001
- Boellaard R, Delgado-Bolton R, Oyen WJ, Giammarile F, Tatsch K, Eschner W, et al. FDG PET/CT: EANM procedure guidelines for tumour imaging: version 2.0. *Eur J Nucl Med Mol Imaging*. (2015) 42:328–54. doi: 10.1007/s00259-014-2961-x
- Sekine T, Delso G, Zeimpekis KG, de Galiza Barbosa F, Ter Voert E, Huellner M, et al. Reduction of (18)F-FDG dose in clinical PET/MR imaging by using silicon photomultiplier detectors. *Radiology*. (2018) 286:249–59. doi: 10.1148/radiol.2017162305
- Gnesin S, Kieffer C, Zeimpekis K, Papazyan JP, Guignard R, Prior JO, et al. Phantom-based image quality assessment of clinical (18)F-FDG protocols in digital PET/CT and comparison to conventional PMT-based PET/CT. *EJNMMI Phys*. (2020) 7:1. doi: 10.1186/s40658-019-0269-4
- Carlier T, Ferrer L, Conti M, Bodet-Milin C, Rousseau C, Bercier Y, et al. From a PMT-based to a SiPM-based PET system: a study to define matched acquisition/reconstruction parameters and NEMA performance of the biograph vision 450. *EJNMMI Phys*. (2020) 7:55. doi: 10.1186/s40658-020-00323-w
- Surti S, Viswanath V, Daube-Witherspoon ME, Conti M, Casey ME, Karp JS. Benefit of improved performance with state-of-the-art digital PET/CT for lesion detection in oncology. *J Nucl Med*. (2020) 61:1684–90. doi: 10.2967/jnumed.120.242305
- Lopez-Mora DA, Flotats A, Fuentes-Ocampo F, Camacho V, Fernandez A, Ruiz A, et al. Comparison of image quality and lesion detection between digital and analog PET/CT. *Eur J Nucl Med Mol Imaging*. (2019) 46:1383–90. doi: 10.1007/s00259-019-4260-z
- Fuentes-Ocampo F, Lopez-Mora DA, Flotats A, Paillahueque G, Camacho V, Duch J, et al. Digital vs. analog PET/CT: intra-subject comparison of the SUVmax in target lesions and reference regions. *Eur J Nucl Med Mol Imaging*. (2019) 46:1745–50. doi: 10.1007/s00259-018-4256-0
- van Sluis J, Boellaard R, Somasundaram A, van Snick PH, Borra RJH, Dierckx R, et al. Image quality and semiquantitative measurements on the biograph vision PET/CT system: initial experiences and comparison with the biograph mCT. *J Nucl Med*. (2020) 61:129–35. doi: 10.2967/jnumed.119.227801
- Kim SH, Song BI, Kim HW, Won KS. Comparison of image quality and semi-quantitative measurements with digital PET/CT and standard PET/CT from different vendors. *Nucl Med Mol Imaging*. (2020) 54:233–40. doi: 10.1007/s13139-020-00661-8
- Hatami S, Frye S, McMunn A, Botkin C, Muzaffar R, Christopher K, et al. Added value of digital over analog PET/CT: more significant as image field of view and body mass index increase. *J Nucl Med Technol*. (2020) 48:354–60. doi: 10.2967/jnmt.120.244160
- Degenhardt C, Rodrigues P, Trindade A, Zwaans B, Mühlens O, Dorscheid R, et al. Performance evaluation of a prototype Positron Emission Tomography scanner using Digital Photon Counters (DPC). In: *2012 IEEE Nuclear Science Symposium and Medical Imaging Conference Record (NSS/MIC)*. Anaheim, CA (2012). p. 2820–4. doi: 10.1109/NSSMIC.2012.6551643

Conflict of Interest: The authors declare that the research was conducted in the absence of any commercial or financial relationships that could be construed as a potential conflict of interest.

Copyright © 2021 Delcroix, Bourhis, Keromnes, Robin, Le Roux, Abgral, Salaun and Querellou. This is an open-access article distributed under the terms of the Creative Commons Attribution License (CC BY). The use, distribution or reproduction in other forums is permitted, provided the original author(s) and the copyright owner(s) are credited and that the original publication in this journal is cited, in accordance with accepted academic practice. No use, distribution or reproduction is permitted which does not comply with these terms.